Impact of Dynamic Online Fed-Batch Strategies on Metabolism, Productivity and N-Glycosylation Quality in CHO Cell Cultures

Danny Chee Furng Wong,[1,2] Kathy Tin Kam Wong,[1] Lin Tang Goh,[1] Chew Kiat Heng,[2] Miranda Gek Sim Yap[1]

*[1]Bioprocessing Technology Institute, Agency for Science and Technology Research (A*STAR), 20 Biopolis Way, #06-01, Centros, Singapore 138668; telephone: 65 6478 8880; fax: 65 6478 9561; e-mail: miranda_yap@bti.a-star.edu.sg*
[2]Department of Pediatrics, National University of Singapore, 10 Kent Ridge Crescent, Singapore 119260

Received 8 March 2004; accepted 25 August 2004

Published online 8 December 2004 in Wiley InterScience (www.interscience.wiley.com). DOI: 10.1002/bit.20317

Abstract: As we pursue the means to improve yields to meet growing therapy demands, it is important to examine the impact of process control on glycosylation patterns to ensure product efficacy and consistency. In this study, we describe a dynamic on-line fed-batch strategy based on low glutamine/glucose concentrations and its impact on cellular metabolism and, more importantly, the productivity and N-glycosylation quality of a model recombinant glycoprotein, interferon gamma (IFN-γ). We found that low glutamine fed-batch strategy enabled up to 10-fold improvement in IFN-γ yields, which can be attributed to reduced specific productivity of ammonia and lactate. Furthermore, the low glutamine concentration (0.3 mM) used in this fed-batch strategy could maintain both the N-glycosylation macro- and microheterogeneity of IFN-γ. However, very low glutamine (<0.1 mM) or glucose (<0.70 mM) concentrations can lead to decreased sialylation and increased presence of minor glycan species consisting of hybrid and high-mannose types. This shows that glycan chain extension and sialylation can be affected by nutrient limitation. In addition to nutrient limitation, we also found that N-glycosylation quality can be detrimentally affected by low culture viability. IFN-γ purified at low culture viability had both lower sialylation as well as glycans of lower molecular masses, which can be attributed to extensive degradation by intracellular glycosidases released by cytolysis. Therefore, in order to maintain good N-glycosylation quality, there is a need to consider both culture viability and nutrient control setpoint in a nutrient-limiting fed-batch culture strategy. A greater understanding of these major factors that affect N-glycosylation quality would surely facilitate future development of effective process controls.

Keywords: CHO; fed-batch; low glutamine; glucose; interferon gamma; glycosylation

Correspondence to: Miranda G. S. Yap

INTRODUCTION

With the completion of the human genome project, more proteins with therapeutic potential are being discovered daily, many of which are glycoproteins. The oligosaccharide structures on these glycoproteins are often critical for a myriad of functions, some of which are crucial for its pharmacokinetic properties (Varki, 1993; Jenkins et al., 1996). The structural heterogeneity of oligosaccharides (glycans) on glycoproteins is sensitive to culture environment including nutrient starvation, metabolic waste accumulation, culture viability, pH, and temperature (Goochee and Monica, 1990; Yang and Butler, 2000; Andersen et al., 2000; Baker et al., 2000). Therefore, even as we pursue the means to improve yields to meet growing therapy demands, it is important to examine the impact of process control on glycosylation patterns to ensure product efficacy and consistency.

As a recombinant glycoprotein production model, a Chinese hamster ovary (CHO) cell line producing recombinant human interferon gamma (IFN-γ) was selected for this study. IFN-γ is a secretory glycoprotein that plays an important immunoregulatory role in host defense against both viral and microbial pathogens (Samuel, 1991; Farrar and Schreiber, 1993; Strichman and Samuel, 2001). CHO cells are the most frequently used mammalian cell lines for recombinant biotherapeutics production. Furthermore, glycan structures of recombinant glycoproteins produced in CHO cells are very similar to those naturally isolated from humans (James et al., 1995; Parekh, 1991; Hooker et al., 1995). IFN-γ contains two N-glycosylation sites at amino acid residues 25 and 97 (Asn25 and Asn97). As IFN-γ glycosylation in CHO cell batch cultures had been well studied, it is an ideal model for comparison with fed-batch systems (Hooker et al., 1995; Yuk and Wang, 2002). The

glycosylation of IFN-γ is critical for proper folding, dimerization, and secretion of the nascent protein (Sareneva et al., 1994). In addition, glycosylated IFN-γ exhibited twice the antiviral activity of its non-glycosylated form. Proper glycosylation also increases circulatory lifetime (Kelker et al., 1983; Saraneva et al., 1995).

Currently, batch and fed-batch cultures continue to be the main culture modes for a vast majority of industrial bioprocesses due to their ease of operation and reliability. The usual practice in batch culture is to supply all the nutrients needed by the cells for the full duration of a run at the beginning of a culture. However, in this approach the cells are subjected to nutrient concentrations much higher than required for energy production and biomass assimilation. The resultant high transport rates of glucose and glutamine coupled with high rates of glycolysis and glutaminolysis results in the production of inhibitory levels of waste metabolites such as lactate and ammonia in animal cells (McKeehan, 1982; Hassel et al., 1991; Lao and Toth, 1997). Thus, fed-batch cultures were developed whereby interval feeding is used to prolong culture life and productivity.

Stoichiometric fed-batch had been successfully employed to optimize CHO cell growth whereby feeding was executed manually using projected cell growth and nutrient demand every 12–24 h (Xie et al., 1997). However, this may lead to high initial fluctuations in nutrient concentrations with each feed, since the feed has to last for 12-24 h. Confinement of the cells to low glucose and glutamine concentrations can result in shifts toward more efficient cellular metabolism with reduced waste production and hence higher cells densities and enhanced production (Glacken et al., 1985; Ljunggren and Haggstrom, 1994; Zhou et al., 1995; Cruz et al., 1999; Europa et al., 2000). Therefore, dynamic nutrient feeding can further tighten the control of these nutrients, resulting in a shift towards a more efficient metabolism (Europa et al., 2000). Lee et al. (2003) recently described the development of an online sampling system to allow continuous online monitoring of glutamine levels to facilitate tight feedback control of glutamine to enable dynamic feeding based on nutrient demand for human embryonic kidney cells (HEK 293) and were successful in improving production. Although N-glycosylation changes during batch and chemostat cultures have been well studied (Goldman et al., 1998; Andersen et al., 2000; Cruz et al., 1999), the impact of metabolic shift and prolonged confinement to low glutamine or glucose during dynamic feeding used for fed-batch cultures on N-glycosylation is relatively unknown.

In this article, the impact of dynamic on-line low glutamine and glutamine/glucose dynamic fed-batch strategies on CHO cell growth and metabolism are described along with their influence on glycosylation quality and heterogeneity. Technical advances now enable the rapid detection of N-glycan heterogeneity using a combination of capillary electrophoresis and mass spectrometry methods (Harmon et al., 1996; Gu and Wang, 1998; Hooker and James, 2000).

MATERIALS AND METHODS

Cell Line and Culture

CHO IFN-γ is a Chinese hamster ovary cell line that had been adapted to grow in suspension. It was originally derived from dehydroxyfolate reductase negative ($DHFR^-$), Dukx cells (Urlaub and Chasin 1980). CHO IFN-γ had been cotransfected with genes for DHFR and human interferon-γ (Scahill et al., 1983). CHO IFN-γ was maintained in glucose/glutamine-free HyQ CHO MPS media (Hyclone, Logan, UT) supplemented with 4 mM glutamine, 20 mM glucose, and 0.25 μM methotrexate (Sigma, St. Louis, MO).

Fed-Batch and Setpoint Control Operations

An initial working volume of 4.0 L of culture media was inoculated with a seeding density of 2.5×10^5 cells/mL in a 5.0 L bioreactor (B. Braun, Melsungen, Germany). Batch cultures were carried out using glucose/glutamine-free HyQ CHO MPS media (Hyclone) supplemented with 20 mM glucose and 4 mM glutamine while fed-batch cultures were supplemented with 4 mM glucose and 0.5 mM glutamine. Dissolved oxygen concentration was maintained at 50% air saturation and culture pH was maintained at 7.15 using intermittent CO_2 addition to the gas mix and/or 7.5% (w/v) $NaHCO_3$ solution (Sigma).

Fed-batch operation was performed using a modified online dynamic feeding strategy (Lee et al., 2003). Online monitoring of concentrations of the relevant controlled nutrient level were conducted every 1.5 h using an automated aseptic online sampling loop. Basal feed media for fed-batch cultures was prepared from a custom-formulated 10× calcium-free, glucose-free, and glutamine-free DMEM/F12 with 1× salts (Hyclone) supplemented with 10 g/L of soybean protein hydrolysate, Hysoy (Quest International, Hoffman Estate, IL), 10 mL/L of chemically defined lipids (Gibco BRL, Grand Island, NY), 1 mg/L of d-biotin (Sigma), 2 mM L-aspartic acid, 2 mM L-asparagine, 4 mM L-cysteine, 1 mM L-glutamic acid, 1 mM L-methionine and 5 mM L-serine (Sigma).

Glutamine-Limited Setpoints

The basal feed media was further supplemented with 100 mM of glutamine (Sigma) and 500 mM of glucose (Sigma). This allowed for glucose to be fed at a molar ratio of 5:1 for every mole of glutamine fed. Every 1.5 h, an automated on-line measurement of residual glutamine concentrations would be taken. If residual glutamine concentration fell below setpoint control concentrations, feed injections would be effected with feed media to raise cul-

Table I. Initial and setpoint concentrations of glucose and glutamine used for batch and fed-batch cultures.

	Batch culture	Fed-batch culture				
		Glutamine limited			Glutamine/glucose limited	
Parameters	No nutrient set-point control implemented	0.1	0.3	0.5	0.3/0.35	0.3/0.70
Initial glutamine	4.0	0.5	0.5	0.5	0.5	0.5
Initial glucose	20.0	4.0	4.0	4.0	4.0	4.0
Glutamine setpoint	None	0.1	0.3	0.5	Profile feeding to maintain glutamine at 0.3 mM	
Glucose setpoint	None	Indirect glucose control through tagging of glucose to glutamine at a molar ratio of 5:1			0.35	0.70

ture glutamine concentrations either to 0.1, 0.3 or 0.5 mM (Table I).

Glucose-Limited Setpoints Coupled With Glutamine-Limited Profile Feeding

This was achieved via the use of two different feed media: a glucose-only concentrate and a glutamine-supplemented basal media. The media used for glutamine profile feeding consisted of basal feed media but only adjusted to 100 mM of glutamine without any glucose. This feed is then supplied to the culture at 1.5-h intervals following a preestablished feed volume based on previous glutamine feeding profiles used to raise culture glutamine concentrations to 0.3 mM. The "decoupled" glucose was supplied to the culture using a separate 440 mM glucose concentrate. Every 1.5 h, an automated on-line measurement of residual glucose was taken. If residual glucose concentration fell below setpoint control concentrations, feed injections of the glucose concentrate were effected to raise culture glucose concentrations either to 0.35 or 0.70 mM (Table I).

Metabolite Analysis

Online metabolite concentrations for either glutamine or glucose were determined via an aseptic online sampling loop connected to a YSI 2700 biochemical analyzer (Yellow Springs Instruments, Yellow Springs, OH) every 1.5 h. In addition, glucose, lactate, glutamine, and glutamate concentrations of off-line samples of culture supernatant collected in 10–16-h intervals were determined using the YSI. Amino acid analysis of the culture was determined using off-line samples by reverse-phase HPLC using a Shimpack VP-ODS column (Shimadzu, Kyoto, Japan). Amino acid derivatization prior to the HPLC analysis was performed using the Waters AccQ Fluor reagent kit (Millipore, Milford, MA). Detection was done at 395 nm with a fluorescent detector (Shimadzu). Ammonia concentrations were determined using a UV spectrophotometric kit (Sigma 117-C).

IFN-γ Quantification

IFN-γ concentrations of serially diluted supernatant samples were analyzed using an enzyme-linked immunosorbent (ELISA) assay (HyCult Biotechnology, Uden, Netherlands). Samples that had the highest IFN-γ concentrations during high viability (>95%) and during low viability (70–80%) were sent for immunoaffinity purification and further N-glycosylation characterization.

Average Specific Rates Calculations

Specific rates for individual metabolite, *x,* were calculated by:

$$\text{Specific rates}, x = \frac{C_2 - C_1}{\int_{t_1}^{t_2} \mathrm{N\ f}(t)\, dt}$$

where C_1 is the concentration of x at an earlier timepoint and C_2 is the concentration of x at the subsequent timepoint and N f(t) is the cell density time profile. A fourth-order polynomial, f(t), is fitted to the cell density data. Average specific rates, q_x, was then calculated across specific growth phases.

Immunoaffinity Purification of IFN-γ

Purified mouse antihuman IFN-γ antibodies from clone B27, 2 mg (BD Pharmingen, San Diego, CA) was coupled to cyanogen bromide-activated Sepharose 4B beads (Amersham Biosciences, Uppsala, Sweden) and then packed into an HR 5/2 0.5 mL column (Amersham Bio-

sciences). Samples containing IFN-γ from culture supernatant were filtered (0.4 μm Millex HV, PVDF low protein binding) (Millipore) and 0.02% sodium azide added. Then 20–40 mL of sample was loaded at 0.2 mL/min into the immunoaffinity column that had been equilibrated with loading buffer (20 mM sodium phosphate buffer, 150 mM NaCl, pH 7.2; Merck, Darmstadt, Germany). Purification was carried out on an AKTA Explorer 100 chromatographic system (Amersham Biosciences). The loading buffer was used to wash the column after loading. The sample was eluted isocratically at 0.02 ml/min using a low pH buffer (10 mM HCl, 150 mM NaCl chloride, pH 2.5; Merck). The column was regenerated for subsequent runs using loading buffer. IFN-γ purified via immunoaffinity has a purity of greater than 98% by reverse phase HPLC and SDS-PAGE (data not shown).

Sialylation Assay

Total sialic acid was measured using the thiobarbituric acid assay adapted from Hammond and Papermaster (1976). Each purified IFN-γ sample (6 μg) was desialylated using 2.5 mU sialidase (Roche, Nutley, NJ) in 50 mM acetate buffer, pH 5.2 (Sigma). The mixture was incubated at 37°C for 24 h. The mixture was then mixed with 250 μL of periodate reagent (25 mM periodic acid in 0.125N H_2SO_4; Sigma) and incubated at 37°C for 30 min. Arsenite solution (200 μL of 2% sodium arsenite in 0.5N HCl) was added to remove excess periodate, followed by the addition of 2 mL of thiobarbituric acid reagent (0.1 M 2-thiobarbituric acid, pH 9.0; Sigma) and incubated at 98°C for 8 min. The samples were cooled on ice for 10 min and then mixed with 1.5 ml of acid/butanol solution (n-butanol containing 5% (v/v) 12N HCl). The samples were shaken vigorously and centrifuged at 3,000 rpm for 3 min. The clear organic phase was transferred to a 10 mm cuvette and the fluorescence intensity ($\lambda_{excitation}$ = 550 nm, $\lambda_{emission}$ = 570 nm) was measured on a Cary Eclipse fluorescence spectrophotometer (Varian, Palo Alto, CA). The sialic acid content of each sample was then quantified in triplicate by interpolating a standard curve generated from pure sialic acid dissolved in water.

IFN-γ Macroheterogeneity: Site Occupancy

The macroheterogeneity or site-occupancy of IFN-γ was determined by micellar electrokinetic capillary chromatography (MECC) using a Beckman Coulter P/ACE MDQ, Capillary Electrophoresis System (Beckman Coulter, Fullerton, CA). A 50 μm i.d. × 50.2 cm length (48 cm to detector) bare silica capillary (Beckman Coulter) was used for separation. Prior to a separation run, the capillary was cleaned with 0.1 M NaOH for 10 min, flushed with HPLC-grade water for 5 min, and subsequently equilibrated with running buffer (100 mM SDS, 30 mM boric acid, 30 mM sodium borate, pH 9; Merck) for another 10 min. Samples were pressure-injected at 5 psi over 5 sec and then a 15 kV voltage was applied to the capillary over 40 min.

Tryptic Digestion and Glycopeptides Separation

Purified IFN-γ (20 μg) was diluted with digestion buffer (50 mM ammonium bicarbonate, pH 8.5) to give a concentration of 0.025 g/μl. Lyophilized TPCK-Trypsin (Sigma) was dissolved in digestion buffer to give a concentration of 0.1 mg/mL. The TPCK-Trypsin solution was then added to give a 1:25 trypsin-to-protein mass ratio. After mixing, the solution was incubated in a water bath for 37°C for 24 h.

Reverse-Phase HPLC separation of IFN-γ Glycopeptides

After tryptic digest, 1.0 mL of the peptide mixture was loaded onto a Vydac 1× 250 mm C_{18} (218TP51) 5 μm particle size column (GraceVydac, Hesperia, CA). Buffer B contained HPLC-grade acetonitrile (Fisher Scientific, Leicestershire UK) and 0.1% (v/v) trifluoroacetic acid (TFA) (Pierce Biotechnology, Rockford, IL) while buffer A contained HPLC-grade water with 0.1% (v/v) TFA. The column was equilibrated at 12% of buffer B for 30 min. The elution of the peptides was performed from 15–35% B over 200 min at 0.05 ml min^{-1}. Peptide peaks were collected for mass spectrometry analysis.

Glycopeptides Analysis Using MALDI/TOF Mass Spectrometry

Glycopeptide fractions (Asn25 and Asn97) collected from reverse-phase HPLC separation were vacuum-dried for 2 h. MALDI/MS was performed on a Voyager DE-STR Biospectrometry system (Applied Biosystems, Foster City, CA) equipped with Voyager v. 5 software (Applied Biosystems). Samples were reconstituted in 20 μL of the 50% acetonitrile solution with 0.1% TFA. Samples were prepared using the thin-layer matrix preparation method (Harvey, 1999) using 1 mL of dihydroxybenzoic acid solution (10 mg/mL 2,5-dihydroxybenzoic acid in 50% acetonitrile, 0.1% TFA solution) and subsequently 1 mL of sample. Ions were accelerated at an acceleration voltage of 20 kV after a delay time of 300–500 nsec. Data for 100 pulses of the 377 nm nitrogen laser were averaged for each spectrum and detected by a reflectron, positive-ion TOF mode.

RESULTS AND DISCUSSION

Establishing a Dynamic On-Line Feedback Control Fed-Batch System

With the aim of tightening the control of nutrient feeding, our group previously developed an on-line direct measure-

ment of glutamine via a continuous cell-exclusion system in human embryonic kidney cells (Lee et al., 2003). A feedback control algorithm can then be applied to maintain glutamine concentrations at levels as low as 0.1 mM with a concentrated feed medium. By adapting the above-mentioned system for CHO cells, several different fed-batch cultures were carried out with different glutamine and glucose setpoint concentrations to determine the impact of dynamic fed-batch strategies on CHO cell growth, metabolism, productivity, and N-glycosylation quality (Table I).

Glutamine was selected over glucose as a setpoint control for two major reasons. First, glutamine is a major source of ammonia, a metabolic waste that affects growth and glycosylation. Glutamine limitation could therefore lower ammonia production and, hence, decrease its detrimental effects on growth and glycosylation (Hassel et al., 1991; Lao and Toth, 1997; Gawlitzek et al., 2000). Second, we have previously found that glucose consumption tends to be significantly higher than glutamine consumption in batch cultures (data not shown). Since our fed-batch strategy requires the confinement of nutrient concentration to low levels, a lower specific consumption rate will allow for greater sensitivity of control, since residual nutrient concentrations would not fluctuate as much. Therefore, glutamine was initially used as a setpoint control instead of glucose. At the same time, to ensure sufficient glucose availability, glucose is tagged to glutamine at a molar ratio of 5:1 following average stoichiometric glucose to glutamine consumption ratio of batch cultures.

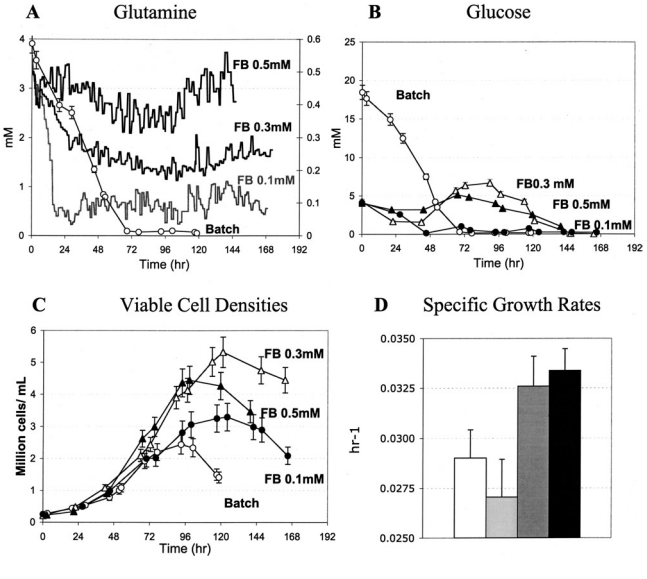

Figure 1. Growth kinetics of glutamine setpoint fed-batch cultures. Concentrations of (**A**) on-line residual glutamine and (**B**) off-line residual glucose with (**C**) viable cell densities of fed-batch cultures controlled at 0.1 mM (●), 0.3 mM (△), and 0.5 mM (▲) glutamine, and control batch (○) culture. **D:** Average specific growth rates, μ, for batch □, glutamine fed-batches at 0.1 mM ▫, 0.3 mM ■, and 0.5 mM ■ (data points represent the averages of two runs).

Effects of Dynamic On-Line Glutamine Control

Glutamine setpoint fed-batch cultures were initiated at lower glutamine and glucose concentrations compared to batch so that feeding could be initiated earlier at ~15–18 h after seeding. Once feeding had been initiated, glutamine concentrations can be maintained at a desired setpoint concentration with moderate fluctuations (Fig. 1A). These fluctuations in residual concentrations are expected, since the specific consumption rates are dynamic, especially across different growth stages. Tagging of glucose to glutamine also allowed residual glucose to be kept at relatively low concentrations (Fig. 1B). This showed that the feeding controls implemented in this dynamic fed-batch system could be quite effective at maintaining a particular setpoint concentration.

All glutamine setpoint fed-batch cultures showed significant improvements in maximum viable cell densities compared to batch culture (Fig. 1C). The use of low glutamine control also did not decrease specific growth rates, μ, during the exponential growth period. However, when glutamine was limited at very low concentration (<0.1 mM), cell growth and maximum viable densities were decreased significantly (Fig. 1C,D). This suggested that glutamine confinement at concentrations lower than 0.1 mM could limit specific growth rates and cell density. Therefore, in order to achieve high cell density and specific growth rate using this fed-batch strategy, glutamine concentrations of greater than 0.3 mM are required.

The higher cell density and prolonged culture life can be attributed not only to increased nutrient availability due to feeding but to significant reduction in ammonia and lactate production as well (Fig. 2A,B). Specific ammonia production, q_{NH4}, of all glutamine fed-batches was lower than that of batch culture (Fig. 3A). Alanine, one of the main overflow metabolites from excessive glutaminolysis, also decreases with increasing glutamine limitation (Fig. 3A). This supported the suggestion by Lee et al. (2003) that lower glutamine levels could restrict overflow of glutamine metabolism through glutaminolysis and

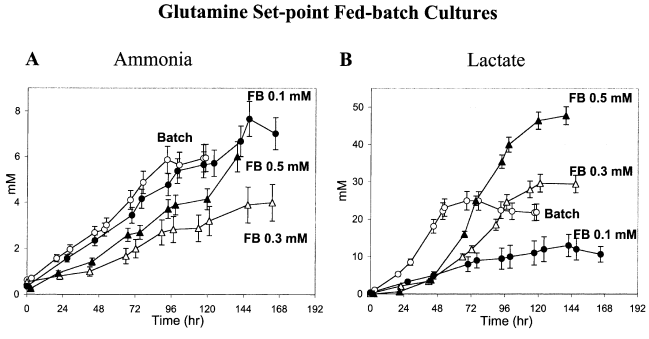

Figure 2. Ammonia and lactate accumulation during batch and fed-batch culture. Concentrations of (**A**) ammonia and (**B**) lactate concentrations during fed-batch cultures controlled at 0.1 mM (●), 0.3 mM (△), and 0.5 mM (▲) glutamine and control batch (○) culture (data points represent the averages of two runs).

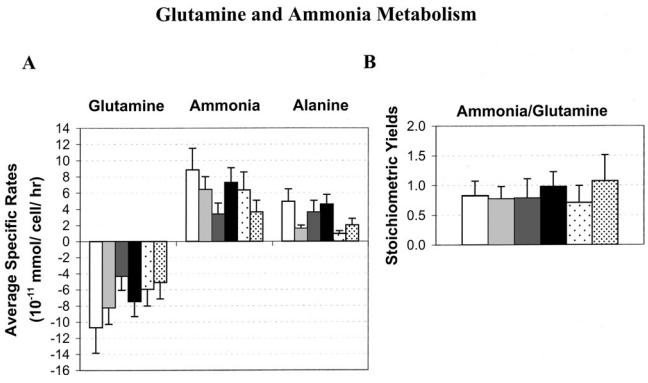

Figure 3. Glutamine and ammonia metabolism. **A:** Average specific glutamine and alanine consumption with ammonia production rates. **B:** Stoichiometric yields of ammonia to glutamine for batch culture □ and glutamine setpoint fed-batch cultures controlled at 0.1 mM ▒, 0.3 mM ▒, and 0.5 mM glutamine ■ and for 0.3 mM/0.35 mM ⁙ and 0.3 mM/0.70 mM ▒ glutamine/glucose fed-batch cultures (data points represent the averages of two runs).

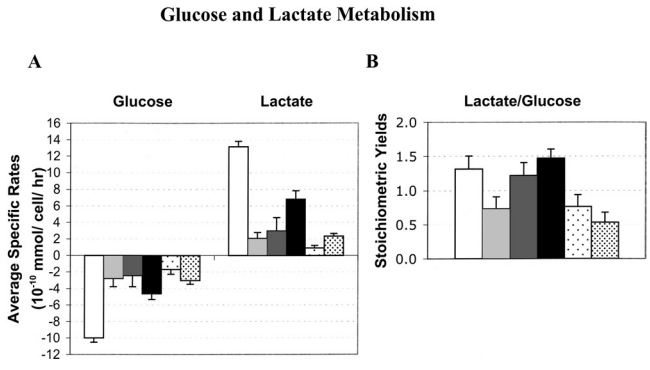

Figure 4. Glucose and lactate metabolism. **A:** Average specific consumption/production rates for glucose and lactate. **B:** Stoichiometric yields of lactate to glucose in batch culture □ and glutamine setpoint fed-batch cultures controlled at 0.1 mM ▒, 0.3 mM ▒, and 0.5 mM ■ glutamine and for 0.3 mM/0.35 mM ⁙ and 0.3 mM/0.70 mM ▒ glutamine/glucose fed-batch cultures (data points represent the averages of two runs).

thereby lower ammonia production. Interestingly, we found that lowered specific ammonia production rates are accompanied by equally lowered glutamine uptake rates. Therefore, ammonia to glutamine yields, $\Delta NH_4/\Delta Gln$, of fed-batch cultures did not differ from that of batch culture (Fig. 3B). It seemed that although this fed-batch method was able to reduce the rate of glutaminolysis, as evidenced by reduced ammonia production, it was unable to increase the efficiency of glutamine metabolism since the absolute amount of ammonia produced per mole of glutamine consumed remained unchanged.

We found that specific ammonia production can be reduced much more significantly by controlling at a lower glutamine concentration of 0.3 mM compared to 0.5 mM (Fig. 3A). However, when glutamine was controlled at a much lower concentration of 0.1 mM, specific ammonia production was increased instead of being reduced further (Fig. 3A). Glutamine consumption was increased as well. It is likely that at 0.1 mM glutamine, glutamine consumption was increased to maintain cellular carbon flux in a severely limited nutrient environment. This is supported by the observation of increased ammonia production, which suggested higher rates of glutaminolysis to provide alternate carbon source. Therefore, for the successful implementation of a dynamic fed-batch strategy it is important to determine a threshold glutamine concentration that is low enough to restrict metabolism overflow and yet high enough to prevent severe nutrient limitation.

In addition, we found that maintaining a fixed glucose-to-glutamine ratio allowed for an indirect method of limiting glucose uptake. Since glucose is being fed gradually by being linked to glutamine, specific glucose consumption decreased significantly (Fig. 4A). Lee et al. (2003) also found that glutamine limitation can decrease glucose uptake rates. This indirect method of restricting glucose uptake enabled specific lactate production to be reduced by as much as 80% (Fig. 4A). Lower glutamine setpoint concentrations also correlate with lower lactate to glucose yields, $\Delta L/\Delta G$ (Fig. 4B). Lowering glutamine setpoint from 0.5 to 0.1 mM resulted in $\Delta L/\Delta G$ decreasing from 1.47 to 0.74. This reduction in glucose conversion to lactate is indicative of a more efficient utilization of glucose (Ljunggren and Haggstrom, 1994).

Effects of On-Line Glucose Control Coupled With Glutamine Profile Feeding

Despite maintaining a fixed ratio of glucose to glutamine at 5:1, the actual consumption ratio typically decreases to ~3:1 with time during fed-batch cultures, as specific glucose consumption typically shows a greater decrease in relation to specific glutamine consumption. This causes glucose overfeeding, as indicated by a gradual increase in residual glucose concentration with time during glutamine setpoint fed-batch cultures (Fig. 1B). As a result of glucose overfeeding, lactate concentration increases significantly, as evidenced by the observation of significant lactate increase coinciding with glucose overfeeding at ~48 h (Fig. 2B).

Previously, we had found that profile feeding using pre-established feed volume profiles for the 0.3 mM glutamine setpoint resulted in growth and production profiles very similar to that of on-line dynamic fed-batch culture (data not shown). This could potentially allow for the removal of the complicated on-line sampling set-up for feeding once feed volumes are established, making this strategy more industrial-friendly. However, scalability of the feeding profile to larger bioreactors would need to be established before it can be translated into a viable production process. Considering the reproducibility of the feeding profile to mimic on-line setpoint control, the same approach was used for the implementation of further glucose control. This will allow for low glucose control and, hence, prevent glucose

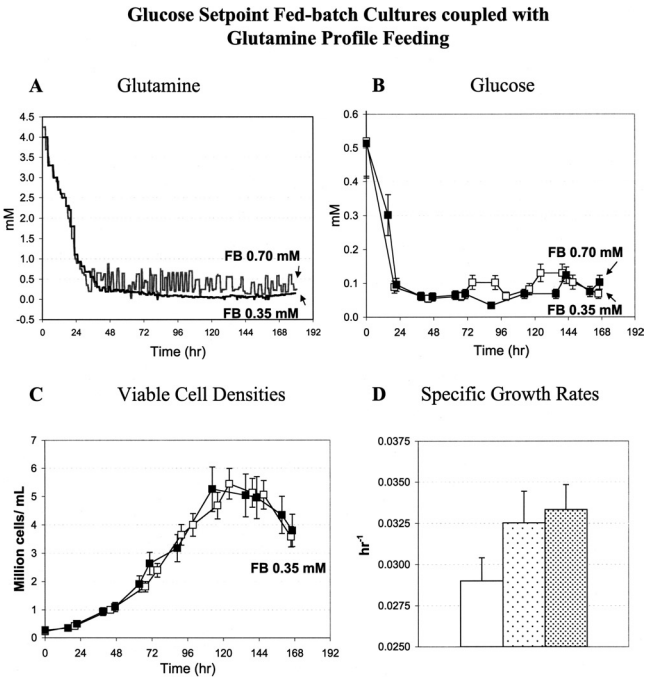

Figure 5. Growth kinetics of glucose setpoint fed-batch cultures coupled with glutamine profile feeding. Concentrations of **(A)** On-line residual glucose and **(B)** Off-line residual glutamine with **(C)** Viable cell densities of fed-batch setpoint cultures controlled at 0.35mM (□) and 0.70mM (■) glucose coupled with glutamine profile feeding. **(D)** Average specific growth rates, μ, for batch □ and fed-batch cultures controlled at 0.35mM ⁙ and 0.70mM ▩ glucose coupled with glutamine profile feeding. (Data points represent the averages of two runs).

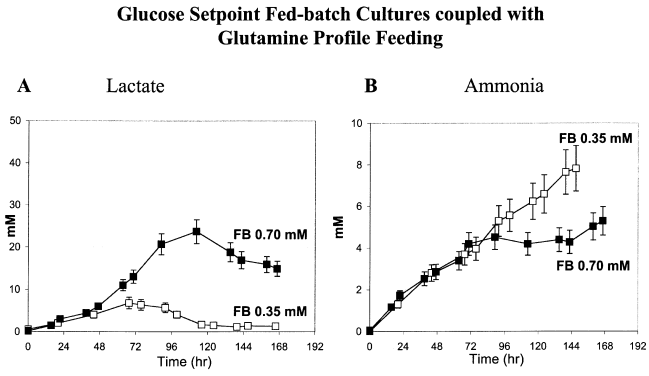

Figure 6. Lactate and ammonia accumulation during glucose setpoint fed-batch cultures coupled with glutamine profile feeding. Lactate (**A**) and ammonia (**B**) concentrations during fed-batch cultures controlled at 0.35 mM (□) and 0.70 mM (■) glucose setpoint coupled with glutamine profile feeding (data points represent the averages of two runs).

overfeeding. To achieve this, glucose was decoupled from the feed media and a separate glucose concentrate was used instead. Through the use of an on-line feedback system, glucose feeding could now be effected to maintain glucose concentration at setpoint concentrations of 0.35 or 0.70 mM every 1.5 h (Fig. 5A).

In spite of additional glucose control in this strategy, comparable maximum viable cell densities and specific growth rates could still be achieved (Fig. 5C,D). Furthermore, there was a further reduction in lactate accumulation (Fig. 6A). By lowering the glucose control concentration from 0.70 to 0.35 mM, $\Delta L/\Delta G$ decreased from 0.76 to 0.53 (Fig. 4B). This indicated that glucose is utilized more efficiently, thereby resulting in lower metabolic waste production. Furthermore, from the residual glucose concentrations of 0.1 mM glutamine setpoint (Fig. 1B) and the glucose/glutamine setpoint fed-batch cultures (Fig. 5B), low $\Delta L/\Delta G$ (<0.8) can only be achieved when residual glucose is kept below 1 mM. When residual glucose was higher than 2 mM, $\Delta L/\Delta G$ was also high (>1.2). This shows that for glucose to be efficiently utilized (low $\Delta L/\Delta G$), residual glucose has to be kept at 1 mM or less. This 1 mM residual glucose observation is consistent with previous work done on BHK cells (Cruz et al., 1999).

Although profile feeding in glutamine/glucose setpoint fed-batch was aimed to simulate setpoint glutamine at 0.3 mM, actual residual glutamine (Fig. 5B) was similar to residual glutamine seen for 0.1 mM glutamine setpoint fed-batch instead (Fig. 1A). This pointed to increased glutamine consumption during implementation of additional glucose control. Indeed, the specific glutamine consumption in the presence of additional glucose control is higher than that of just 0.3 mM glutamine control alone (Fig. 3A). This suggested that more glutamine is utilized when glucose availability is reduced. This in turn increased ammonia accumulation to levels typically seen for batch culture (Fig. 6B). Glutamine is one of the major intermediates of the anaplerotic pathways that provide alternative carbon sources that help maintain the carbon flux in the tricarboxylic acid (TCA) cycle for energy production. This involves the deamination of glutamine to glutamate before conversion to 2-oxoglutarate, an intermediate of the TCA cycle. This results in the formation of ammonia as a secondary metabolite. It is likely that under low glucose limitations the cells utilize extra glutamine to maintain carbon flux, resulting in the observed lower residual glutamine as

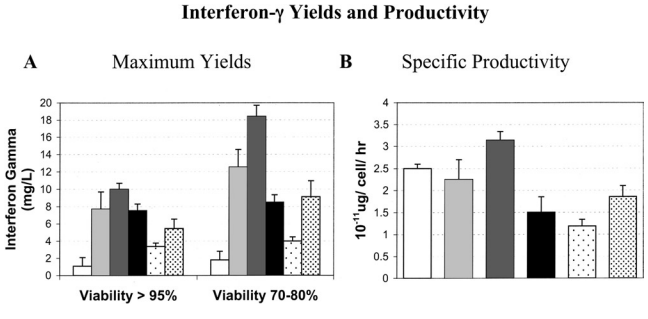

Figure 7. Recombinant human IFN-γ production in CHO cells during batch and fed-batch cultures. **A:** Average specific IFN-γ productivity rates. **B:** Maximum IFN-γ yields during high and low viability for batch culture □ and glutamine setpoint fed-batch cultures controlled at 0.1 mM ▩, 0.3 mM ▩, and 0.5 mM ■ glutamine and for 0.3 mM/0.35 mM ⁙ and 0.3 mM/0.70 mM ▩ glutamine/glucose fed-batch cultures (data points represent the averages of two runs).

well as higher specific ammonia production compared to fed-batch cultures without additional glucose control.

Recombinant IFN-γ Yield and Productivity of CHO Cells

We found that glutamine setpoint fed-batch cultures could significantly improve IFN-γ yield compared to batch culture (Fig. 7A,B). The greatest improvement in yields could be observed in 0.3 mM followed by 0.1 mM and 0.5 mM glutamine setpoint fed-batch cultures. Up to a 10-fold increase in IFN-γ yield can be achieved by the use of optimal low glutamine setpoint control of 0.3 mM (Fig. 7A). With the exception of 0.3 mM glutamine setpoint, specific IFN-γ productivity, $q_{IFN\text{-}\gamma}$ of glutamine setpoint fed-batch cultures was lower than that of batch (Fig. 7B). At lower glutamine setpoint, 0.1 mM, maximum viable cell density and $q_{IFN\text{-}\gamma}$ were lower, probably due to nutrient limitation, while at higher glutamine setpoint, 0.5 mM, higher ammonia and lactate accumulation probably decreased $q_{IFN\text{-}\gamma}$ as well as viable culture time. It is clear that although glutamine limitation can improve the efficiency of cellular metabolism, an optimal concentration threshold must be determined.

Interestingly, despite the ability of additional glucose control in achieving comparable high viable cell densities and lowering lactate accumulation at the same time, IFN-γ yields were much lower than that of just glutamine control alone (Fig. 7A). When glucose was controlled at 0.70 mM, IFN-γ yields were only ~50% that of without glucose control, while 0.35 mM glucose control reduced IFN-γ yield detrimentally to the low yields typically seen in batch culture. It is likely that under these glutamine/glucose limited conditions, cellular metabolism could maintain cell growth but not recombinant protein production due to carbon starvation. This is supported by the observation of lowered $\Delta L/\Delta G$ coupled with increased $\Delta NH_4/\Delta Gln$, showing a more efficient use of glucose, but higher glutamine requirement at the same time to maintain the carbon flux.

Determining N-Glycosylation Quality of IFN-γ

The N-linked glycosylation pathway has been widely studied and it is accepted that a key feature of the process is that individual glycosylation reactions do not always proceed to completion, leading to the secretion of a mixture of differently glycosylated products (Kornfeld and Kornfeld, 1985). MECC methods allow for high-resolution separation of the three site-occupancy variants of IFN-γ, 2N, 1N, and 0N (James et al., 1994; Harmon et al., 1996). Using this method, no significant differences could be observed in the glycan macroheterogeneity of IFN-γ (Fig. 8A). Analysis of the glycans of IFN-γ at different sites was performed by reversed phase peptide/glycopeptide mapping and mass spectrometry (Harmon et al., 1996). The high sensitivity of this method allowed for the detection of many components caused by glycan microheterogeneity.

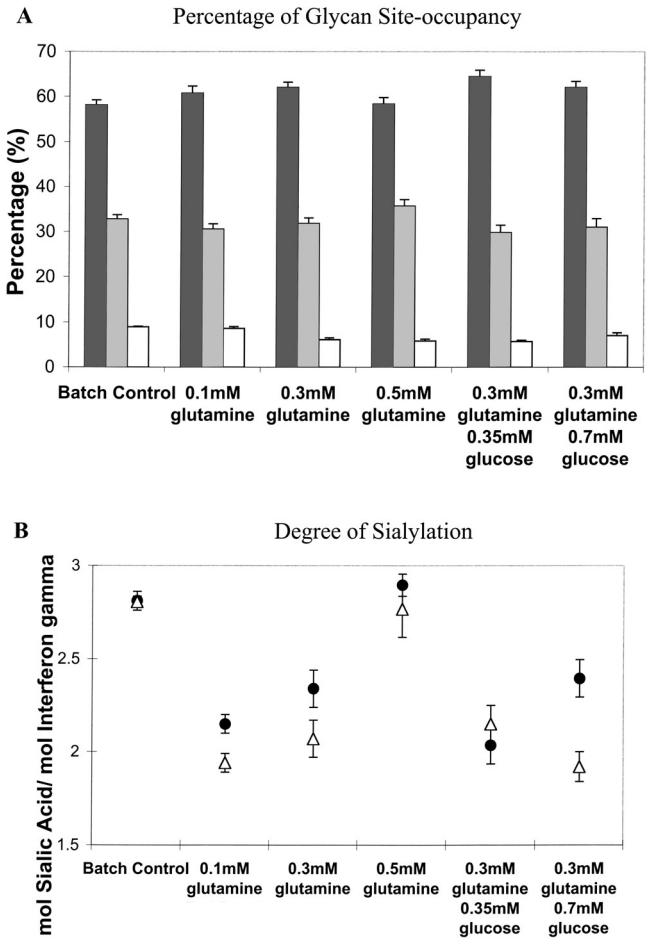

Figure 8. Glycan site-occupancy and sialylation of IFN-γ in batch and fed-batch culture. **A:** Proportion of 2-N ■, 1-N ▒, and 0-N □ glycan site-occupied IFN-γ in batch and fed-batch cultures. **B:** Sialic acid content of maximum IFN-γ harvested during high viability, >95% (●) and low viability, 70–80% (△) in batch and fed-batch cultures (data points represent the averages of two runs).

Site-Occupancy of IFN-γ Glycans (Macroheterogeneity)

MECC data showed no significant differences in the glycan site-occupancy of IFN-γ molecules harvested during high viability. The 2N species, where glycans are present on both the Asn25 and Asn97 N-glycosylation sites of IFN-γ, are the predominant form, making up to 58–64% of all IFN-γ molecules, while 30–35% are 1N species. Unglycosylated species constituted only about 6–9% of all IFN-γ molecules (Fig. 8A). The results obtained here showed that the use of glutamine/glucose limitations does not cause any significant effects on the macroheterogeneity distribution of IFN-γ molecules. This is in contrast to previous findings that showed a decrease in site glycosylation occupancy during low glucose or glutamine concentrations (Hayter

Table II. Sugar compositions and glycan structure of Asn25.

Glycan type	ID	Sugar compositions	Glycan mass	
			Detected	Expected
High mannose	M04	Man_7 $GlcNAc_2$	3793.3	3792.7
	M05	Man_8 $GlcNAc_2$	3955.3	3954.7
	M07	Man_{10} $GlcNAc_2$	4279.9	4278.8
	M08	Man_{11} $GlcNAc_2$	4441.9	4440.9
Hybrid	H02	Gal_1 Man_5 $GlcNAc_3$	3835.0	3833.7
	H04	Gal_1 Man_6 $GlcNAc_3$	3996.7	3995.7
	H03-F	$NeuAc_1$ Gal_1 Man_4 $GlcNAc_3$ Fuc_1	4109.8	4108.8
	H06-F	$NeuAc_1$ Gal_1 Man_5 $GlcNAc_3$ Fuc_1	4270.4	4270.8
Complex bi-antennary	C03-F	Man_3 $GlcNAc_4$ Fuc_1	3697.1	3696.7
	C04-F	Gal_1 Man_3 $GlcNAc_4$ Fuc_1	3860.4	3858.7
	C07-F	Gal_2 Man_3 $GlcNAc_4$ Fuc_1	4021.8	4020.8
	C10-F	$NeuAc_1$ Gal_1 Man_3 $GlcNAc_4$ Fuc_1	4149.4	4149.8
	C13-F	$NeuAc_1$ Gal_2 Man_3 $GlcNAc_4$ Fuc_1	4310.5	4311.9
	C21-F	$NeuAc_2$ Gal_2 Man_3 $GlcNAc_4$ Fuc_1	4603.7	4603.0
Complex tri-antennary	C05-F	Man_3 $GlcNAc_5$ Fuc_1	3900.2	3899.7
	C08-F	Gal_1 Man_3 $GlcNAc_5$ Fuc_1	4060.5	4061.8
	C14-F	$NeuAc_1$ Gal_1 Man_3 $GlcNAc_5$ Fuc_1	4353.1	4352.9
	C22-F	$NeuAc_1$ Gal_3 Man_3 $GlcNAc_5$ Fuc_1	4677.5	4677.0
	C27-F	$NeuAc_2$ Gal_3 Man_3 $GlcNAc_5$ Fuc_1	4968.7	4968.1
Complex tetra-antennary	C09-F	Man_3 $GlcNAc_6$ Fuc_1	4104.3	4102.8
	C16-F	Gal_2 Man_3 $GlcNAc_6$ Fuc_1	4425.4	4426.9

Assignment of sugar compositions and structures are based on glycan mass determined from mass spectrometry. Residues: *N*-acetylglucosamine (GlcNAc), fucose (Fuc), mannose (Man), galactose (Gal), and *N*-acetylneuramic acid (NeuAc). An alphanumeric ID is assigned to each structure type, high-mannose (M), hybrid (H), complex (C), fucosylated (F), and higher numeric values denote higher molecular masses.

et al., 1992; Xie et al., 1997; Nyberg et al., 1999). Nyberg et al. (1999) suggested that the decrease could be attributed to a decrease in intracellular UDP-GalNAc and UDP-GlcNAc availability detected during glucose or glutamine limitation. However, despite a 40% decrease in nucleotide sugars, site-occupancy only decreased from 72% to 62% 2-N species (Nyberg et al., 1999). Therefore, it seems that only extreme starvation would lead to a decrease in glycan site-occupancy. It may be that, compared to conventional fed-batch feeding (once every 12–24 h), the use of dynamic feeding (once every 1.5 h) could maintain intracellular pools of nucleotide sugars at sufficient levels without impacting glycosylation site-occupancy since periods of extreme starvation can be kept to a minimum.

Structure and Composition of Interferon-γ Glycans (Microheterogeneity)

Tables II and III show the structure and sugar compositions of oligosaccharides attached to Asn25 and Asn97 of IFN-γ, respectively. A reference alphanumeric ID is given to each glycan denoting high-Mannose (M), Hybrid (H), and Complex (C) types, Fucosylated (F) glycans; with higher numerical values indicating higher glycan molecular weights. Approximate estimates of relative abundance of different glycan forms can be obtained by comparison of the relative signal intensities in the mass spectrometry spectra (Sareneva et al., 1996).

In batch culture, the glycans of both Asn25 and Asn97 are mainly complex types, but those of Asn25 are mainly fucosylated, while that of Asn97 are unfucosylated. The complex bi-, tri-, and tetra-antennary oligosaccharides detected are either fully sialylated or lack either sialic acid or sialic acid and galactose on one or more branches. The major species for Asn25 is C08-F, a fucosylated complex tri-antennary glycan (Table IV), while Asn97 has two major species, C07 and C13, both of which are unfucosylated complex bi-antennary glycans (Table V).

Examination of the microheterogeneity of glycans on Asn25 and Asn97 showed that the major species of both sites are relatively unaffected by glutamine limitation (Tables IV, V). However, on Asn25 we detected several hybrid types (H02, H04, H03-F, and H06-F) and one extra high-mannose type (M07) glycans, which was absent in IFN-γ produced in batch cultures (Table IV). With Asn97, there were less complex tri- and tetra-antennary complex types observed (Table V). Again, there was an increase in hybrid types (H02 and H03) but no extra high-mannose could be detected. Interestingly, another major species appeared at 0.3 and 0.5 mM glutamine setpoint control, C08, a complex tri-antennary glycan. Several high molecular weight complex tri- and tetra-antennary glycans could

Table III. Sugar compositions and glycan structure of Asn97.

Glycan type	ID	Sugar compositions	Glycan mass	
			Detected	Expected
High mannose	M01	Man_4 $GlcNAc_2$	2577.4	2577.1
	M02	Man_5 $GlcNAc_2$	2739.7	2739.2
	M04	Man_7 $GlcNAc_2$	3063.9	3063.3
	M05	Man_8 $GlcNAc_2$	3226.1	3225.4
	M07	Man_{10} $GlcNAc_2$	3550.6	3549.5
	M08	Man_{11} $GlcNAc_2$	3712.7	3711.5
Hybrid	H02	Gal_1 Man_5 $GlcNAc_3$	3105.0	3104.3
	H03	$NeuAc_1$ Gal_1 Man_4 $GlcNAc_3$	3233.9	3233.3
	H06	$NeuAc_1$ Gal_1 Man_5 $GlcNAc_3$	3396.4	3395.4
Complex bi-antennary	C01	Man_3 $GlcNAc_3$	2618.9	2618.2
	C02	Gal_1 Man_3 $GlcNAc_3$	2781.3	2780.2
	C03	Man_3 $GlcNAc_4$	2822.3	2821.2
	C04	Gal_1 Man_3 $GlcNAc_4$	2983.0	2983.3
	C07	Gal_2 Man_3 $GlcNAc_4$	3147.1	3145.4
	C10	$NeuAc_1$ Gal_1 Man_3 $GlcNAc_4$	3275.4	3274.4
	C13	$NeuAc_1$ Gal_2 Man_3 $GlcNAc_4$	3437.6	3436.4
	C21	$NeuAc_2$ Gal_2 Man_3 $GlcNAc_4$	3729.1	3727.5
Complex tri-antennary	C05	Man_3 $GlcNAc_5$	3025.7	3024.3
	C08	Gal_1 Man_3 $GlcNAc_5$	3184.8	3186.4
	C11	Gal_2 Man_3 $GlcNAc_5$	3349.6	3348.4
	C14	$NeuAc_1$ Gal_1 Man_3 $GlcNAc_5$	3476.6	3477.5
	C15	Gal_3 Man_3 $GlcNAc_5$	3512.1	3510.5
	C22	$NeuAc_1$ Gal_3 Man_3 $GlcNAc_5$	3803.1	3801.6
Complex tetra-antennary	C09	Man_3 $GlcNAc_6$	3226.3	3227.4
	C16	Gal_2 Man_3 $GlcNAc_6$	3552.3	3551.5
	C20	Gal_3 Man_3 $GlcNAc_6$	3712.4	3713.6

Assignment of sugar compositions and structures are based on glycan mass determined from mass spectrometry. Residues: *N*-acetylglucosamine (GlcNAc), fucose (Fuc), mannose (Man), galactose (Gal), and *N*-acetylneuramic acid (NeuAc). An alphanumeric ID is assigned to each structure types, high-mannose (M), hybrid (H), complex (C), fucosylated (F), and higher numeric values denotes higher molecular masses.

no longer be observed on both Asn25 and Asn97. This shows that glutamine limitation can affect the complete processing of high-mannose types to full complex types resulting in hybrid types and decreases the efficiency of sugar addition on large bi- and tri-antennary complex glycans.

Implementation of additional glucose control did not have any significant impact on the major glycan species of Asn25 and Asn97, as the dominant species are still C08-F for Asn25 (Table IV) and C07 and C13 for Asn97 (Table V). However, many minor complex type species (C03-F, C04-F, C07-F, C10-F, C21-F, C22-F, C27-F, and C09-F) could no longer be observed at Asn25 and a greater number of high-mannose type glycans (M01, M04, M05, M07) were observed at both Asn25 and Asn97. The glycans of Asn97 have less complex tri- and tetra-antennary structures (C11, C14, C20, C23), which extended beyond GlcNAc (Table V). Table IV shows that many of the higher molecular weight glycan species could no longer be observed with low glucose control.

The addition of glucose limitation to glutamine control seems to further impair the processing of high-mannose to complex type glycans, as seen by an obvious increase in high-mannose type oligosaccharides for both Asn25 and Asn97. It has been demonstrated that the proportion of high-mannose oligosaccharides increase during batch culture as well (Hooker et al., 1995). Hooker et al. (1999) suggested that limitations in glycoprotein transport from endoplasmic reticulum to *cis*-golgi caused the premature release of high-mannose glycoproteins. Since the $q_{IFN\text{-}\gamma}$ is typically lower in glutamine/glucose-limited fed-batch, transport limitation could not have been the cause of high-mannose glycan increase observed in fed-batch. Instead, we hypothesize that glucose and glutamine limitation leads to a decrease in UDP-GlcNAc availability, thereby impairing intracellular glycosylation. It has been shown that glutamine limitation does limit UDP-GlcNAc formation (Nyberg et al., 1999).

Sialylation of Recombinant IFN-γ

Regardless of the identity of the terminating sugar on a glycan, there are a multitude of receptors that will recognize the different oligosaccharides for clearance in vivo (Varki, 1993). The most important and crucial determinant of circulatory half-life in vivo and, thus, the pharmacokinetic

Table IV. Microheterogeneity if IFN-γ glycans on Asn25 harvested during high viability (>95%).

			Fed-batch				
			Glutamine (mM)			Glutamine/ glucose (mM)	
Asn25	ID	Batch	0.1	0.3	0.5	0.3/0.35	0.3/0.70
High mannose	M04						+
	M05					+	+
	M07		+	+	+	+	
	M08	+	+	+	+	+	
Hybrid	H02				+	+	
	H04				+	+	+
	H03-F		+	+	+	+	+
	H06-F		+	+			
Complex	C03-F	+	+	+	+		
(bi-antennary)	C04-F	+	+	+	+		
	C07-F	+	+	+	+		
	C10-F	+	+	+	+		
	C13-F	+	+	+	+	+	+
	C21-F	+		+	+		
Complex	C05-F			+	+		
(tri-antennary)	C08-F	+++++	+++	+++	+++	+++	+++++
	C14-F	+	+	+	+	+	+
	C22-F	+					
	C27-F	+		+	+		
Complex	C09-F	+		+	+		
(tetra-antennary)	C16-F	+	+	+	+	+	+

Approximate quantification was obtained using relative peak intensity of mass spectometry (+: 5–30%, +++: 30–60%, +++++: 60–90%).

Table V. Microheterogeneity if IFN-γ glycans on Asn97 harvested during high viability (>95%).

			Fed-batch (mM)				
			Glutamine			Glutamine/ glucose	
Asn97	ID	Batch	0.1	0.3	0.5	0.3/0.35	0.3/0.70
High mannose	M01					+	
	M02	+	+	+	+	+	+
	M04					+	+
	M05					+	+
	M07					+	+
	M08	+	+	+	+	+	
Hybrid	H02			+	+	+	
	H03	+		+	+	+	
	H06	+	+	+	+	+	+
Complex	C01	+	+	+	+	+	+
(bi-antennary)	C02	+	+	+	+	+	+
	C03			+	+	+	+
	C04	+	+	+	+	+	+
	C07	+++	+++	+++++	+++	+++++	+++++
	C10	+	+	+	+	+	+
	C13	+++	+++	+++	+++	+++	+++
	C21	+	+	+	+	+	+
Complex	C05			+	+	+	+
(tri-antennary)	C08		+	+++	+++	+	
	C11	+	+	+	+		
	C14	+	+	+	+		
	C15	+	+	+	+	+	+
	C22	+	+	+	+	+	+
Complex	C09	+				+	+
(tetra-antennary)	C16	+	+	+	+	+	
	C20	+		+	+		
	C23	+	+	+	+		

Approximate quantification was obtained using relative peak intensity of mass spectrometry: (+: 5–30%, +++: 30–60%, +++++: 60–90%).

properties of the biotherapeutic is the sialylation of an N-glycan. It is therefore particularly important to ensure that process development not only improves yield but maintains high degree of sialylation as well.

We found that typically IFN-γ from batch cultures contained an average of 2.8 mol sialic acid / mol IFN-γ (Fig. 8B). IFN-γ harvested from 0.5 mM glutamine setpoint fed-batch during high viability has a comparable sialic acid content of 2.9 mol sialic acid / mole IFN-γ; however, with further glutamine limitation, sialic acid content decreased significantly. At 0.3 mM glutamine, sialic acid content decreased by 17%, while 0.1 mM glutamine setpoint fed-batch decrease by 23% when compared to batch culture. The addition of glucose control also did not improve sialylation, but rather decreased sialylation, especially at lower glucose control.

The observed decrease in sialylation in fed-batch could be due to a multiplicity of factors, but since the IFN-γ was harvested at high viability it is unlikely that released cytosolic sialidase is responsible for the reduced sialylation. Sialylation decrease could either be due to impaired sialyltransferases activity, low concentrations of substrate, or nucleotide-sugar donor, CMP-NeuAc. Nyberg et al. (1999) found that glutamine limitation can limit the formation of UDP-GlcNAc by limiting amino sugar formation. UDP-GlcNAc is essential for the formation of *N*-acetylmannosamine (ManNAc), a direct precursor of CMP-NeuAc (Pels Rijcken et al., 1995). However, earlier on we hypothesized that the use of dynamic feeding could maintain nucleotide sugar concentrations since glycosylation site-occupancy is not affected by glucose or glutamine limitation. Since sialylation is the final terminal step of N-glycosylation, it would probably be more sensitive to substrate depletion. Another obvious cause of sialylation decrease could be a decreased number of complex species as well as molecular weight of complex glycans observed with glucose/glutamine limitation (Tables IV, V). Therefore, less complex type glycans are available for sialylation and, at the same time, the lower molecular masses meant that most of these complex glycans lack the necessary sugar chain extension for sialylation to proceed.

Despite the lowered sialic acid content of low glutamine or glucose setpoint fed-batch, its high IFN-γ yield makes it an attractive process for further development. Precursor feeding strategies could very well be effective in increasing its sialic acid content. The addition of 20 mM of ManNAc to CHO cells culture has been shown to be effective in improving sialylation by increasing intracellular CMP-NeuAc availability (Gu and Wang, 1998).

Impact of Culture Viability on N-glycosylation Quality

Although viability of fed-batch cultures typically dropped at around 96–120 h, IFN-γ production yields can still be improved by 2–10 times (Fig. 7A). However, degradative enzymes released during cell lysis could have detrimental effects on glycoprotein quality. We found that glycan site-occupancy of IFN-γ molecules harvested at low viability had very similar distribution to that of those harvested at high viability (Fig. 8A). This showed that harvesting at low viability had little impact on the macroheterogeneity of IFN-γ.

However, when the microheterogeneity of IFN-γ glycans were examined, it was found that glycan species from low viability-harvested IFN-γ tend to have lower molecular weight (Tables VI, VII). Generally, there were decreases in higher molecular weight glycan species coupled with increases in low molecular weight glycan species detected on Asn25 and Asn97 in both batch and fed-batch cultures. However, major glycan species, C08-F on Asn25 (Table IV) and C07 on Asn97 (Table V), was maintained despite viability drops. If this was due to synthesis efficiency defects, the previously high molecular weight glycans detectable at high viability, which have already been synthesized, should still be detectable at low viability. Since these high molecular weight species could no longer be detected, they were probably degraded. This suggested that extracellular glycosidases could be degrading the glycans leading to shorter glycans of lower molecular weight. Losses in high molecular weight glycan species appears to be lower in batch and in 0.3/0.35 mM glutamine/glucose fed-batch where IFN-γ yields were low. This suggests that degradation is not as significant with low IFN-γ yields.

When culture viability decreased, we found that IFN-γ sialic acid content decreased as well. IFN-γ molecules harvested at lower viability tend to have lower sialic acid content compared to those harvested at higher viability (Fig. 8B). Approximately 10–20% decrease in mol sialic acid/mol IFN-γ could be detected with viability drop. Sialic acid loss did not appear to be an issue where IFN-γ yields were low, as seen by the relatively unchanged sialic acid content for batch and 0.3/0.35 mM glutamine/glucose setpoint fed-batch. Gramer and Goochee (1993) identified sialidase activity in CHO cell supernatant that has optimum activity at pH 5.5 but still has significant activity at pH 7.0. Since the pH of the reactor is controlled at 7.15, intracellular sialidase released into culture supernatant would still have significant desialylation activity. Previous work by Gu and Wang (1998) and Goldman et al. (1998) showed that an increase in sialidase activity followed viability loss closely in perfusion and stirred-tank CHO cell culture and sialylation was stable until the onset of cell death and lysis. We too have found that sialidase activity in culture supernatant increases with viability loss (data not shown).

Table VI. Microheterogeneity of IFN-γ glycans on Asn25 harvested during low viability (70–80%).

			Fed-batch (mM)				
			Glutamine			Glutamine/glucose	
Asn25	ID	Batch	0.1	0.3	0.5	0.3/0.35	0.3/0.70
High mannose	M04						+
	M05		+	+		+	+
	M07				+	+	
	M08		+	+	+		
Hybrid	H02						+
	H04						
	H03-F					+	+
	H06-F						+
Complex	C03-F						
(bi-antennary)	C04-F						+
	C07-F	+			+		
	C10-F	+	+	+	+		+
	C13-F	+	+	+	+	+	
	C21-F			+			
Complex	C05-F						
(tri-antennary)	C08-F	+++	+++++	+++++	+++++	+++++	+++++
	C14-F	+	+	+	+	+	+
	C22-F	+		+	+		
	C27-F			+			
Complex	C09-F	+		+	+		
(tetra-antennary)	C16-F		+	+	+	+	+

Approximate quantification was obtained using relative peak intensity of mass spectrometry: (+: 5–30%, +++: 30–60%, +++++: 60–90%).

Table VII. Microheterogeneity of INF-γ glycans on Asn97 harvested during low viability (70–80%).

			Fed-batch (mM)				
			Glutamine			Glutamine/ glucose	
Asn97	ID	Batch	0.1	0.3	0.5	0.3/0.35	0.3/0.70
High mannose	M01		+			+	
	M02	+	+	+	+	+++	+++
	M04						
	M05	+		+	+	+	+
	M07					+	+
	M08	+		+	+	+	+
Hybrid	H02					+	+
	H03						
	H06	+	+	+	+	+	+
Complex	C01		+	+	+	+	+
(bi-antennary)	C02	+	+	+	+	+	+
	C03		+	+++	+	+++	+
	C04	+	+	+	+	+	+
	C07	+++	+++	+++	+++	+++++	+++++
	C10	+	+	+	+	+	+
	C13	+++	+	+++	+	+++	+++
	C21	+		+	+	+	+
Complex	C05			+	+	+	+
(tri-antennary)	C08	+	+	+++	+++		
	C11			+	+		
	C14	+		+	+		
	C15	+	+	+	+	+	+
	C22	+	+	+	+	+	+
	C09	+				+	+
Complex	C16	+	+	+	+	+	
(tetra-antennary)	C20	+		+	+		
	C23	+	+	+	+		

Approximate quantification was obtained using relative peak intensity of mass spectrometry: (+: 5–30%, +++: 30–60%, +++++: 60–90%).

These findings suggest that release of intracellular sialidase during cell death contributes significantly to sialic acid removal from sialylated N-glycans harvested. To prevent this, sialidase inhibitors can be added prior to cell lysis to prevent loss of sialic acid significantly (Gramer and Goochee, 1993; Gramer et al., 1995; Gu and Wang, 1998). This method, however, is not ideal for bioprocesses, as it involves the addition of extra chemicals during a process. Simpler alternatives to prevent sialic acid loss include optimization of media to prolong viability or termination of the culture prior to cell lysis especially if limited yield increase does not justify prolonging culture life.

CONCLUSIONS

Experimental data presented here demonstrate that dynamic glutamine or glutamine/glucose controls are effective strategies for enhancing cellular metabolism by decreasing metabolite waste production. This ultimately leads to higher viable cell density and prolonged viability, causing significant increases in glycoprotein productivity and yield. Feeding volumes recorded during glutamine setpoint fed-batch could also be utilized for profile feeding, thereby removing the need for complicated on-line control systems. However, these strategies do influence glycoprotein quality significantly, especially in terms of N-glycan microheterogeneity distribution and sialylation degree. It is obvious that the cell culture variables that affect glycosylation are as varied as they are complex. There is a need to consider possible extracellular factors that can influence enzyme activity or substrate availability as well as possible extracellular modification by cytolysis-associated glycosidases during process development for glycoprotein production.

NOMENCLATURE

CHO	Chinese hamster ovary
IFN-γ	Recombinant human interferon gamma
MECC	Micellar electrokinetic capillary electrophoresis
MALDI/TOF	Matrix-assisted laser desorption ionization / time of flight mass spectroscopy
q_x	Average specific consumption/production of x
Man	Mannose
NeuAc	*N*-acetylneuraminic acid
Gal	Galactose
Fuc	Fucose
GlcNAc	*N*-acetylglucosamine
ManNAc	*N*-acetylmannoside
UDP	Uridine 5′-diphosphate
CMP	Cytidine monophosphate

The authors thank Goh Kian Mau, Mao Yan Ying, Wong Chun Loong, Lee Yih Yean, and Gary Khoo for excellent technical assistance.

References

Andersen DC, Bridges T, Gawlitzek M, Hoy C. 2000. Multiple cell culture factors can affect the glycosylation of Asn-184 in CHO-produced tissue-type plasminogen activator. Biotechnol Bioeng 70:25–31.

Baker KN, Rendall MH, Hills AE, Hoare M, Freedman RB, James DC. 2001. Metabolic control of recombinant protein N-glycan processing in NS0 and CHO cells. Biotechnol Bioeng 73:188–202.

Cruz HJ, Moreira JL, Carrondo MJT. 1999. Metabolic shifts by nutrient manipulation in continuous cultures of BHK cells. Biotechnol Bioeng 66:104–108.

Europa AF, Gambhir A, Fu PC, Hu WS. 2000. Multiple steady states with distinct cellular metabolism in continuous culture of mammalian cells. Biotechnol Bioeng 67:25–34.

Farrar MA, Schreiber RD. 1993. The molecular cell biology of interferon-gamma and its receptor. Annu Rev Immunol 11:571–611.

Gawlitzek M, Ryll T, Lofgren J, Sliwkowski MB. 2000. Ammonium alters N-glycan structures of recombinant TNFR-IgG: degradative versus biosynthetic mechanisms. Biotechnol Bioeng 68:637–646.

Glacken MW, Fleischaker RJ, Sinskey AJ. 1985. Reduction of waste secretion via nutrient control: possible strategies for maximizing product and cell yields on serum in cultures of mammalian cells. Biotechnol Bioeng 28:1376–1389.

Goldman MH, James DC, Rendall M, Ison AP, Hoare M, Bull AT. 1998. Monitoring recombinant human interferon-gamma N-glycosylation during perfused fluidized-bed and stirred-tank batch culture of CHO cells. Biotechnol Bioeng 60:596–607.

Goochee CF, Monica T. 1990. Environmental effects on protein glycosylation. Biotechnology 8:421–427.

Gramer MJ, Goochee CF. 1993. Sialidase activities in Chinese hamster

ovary cell lysate and cell culture supernatant. Biotechnol Prog 9: 366–373.
Gramer MJ, Goochee CF, Chock VY, Brousseau DT, Sliwkowski MB. 1995. Removal of sialic acid from a glycoprotein in CHO cell culture supernatant by the action of an extracellular CHO cell sialidase. Bio/Technol 13:692–698.
Gu X, Wang DIC. 1998. Improvement of interferon-gamma sialylation in Chinese hamster ovary cell culture by feeding of N-acetylmannosamine. Biotechnol Bioeng 58:642–648.
Hammond KS, Papermaster DS. 1976. Fluorometric assay of sialic acid in the picomole range: a modification of thiobarbituric acid assay. Anal Biochem 74:292–297.
Harmon BJ, Gu X, Wang DIC. 1996. Rapid monitoring of site-specific glycosylation microheterogeneity of recombinant human interferon-γ. Anal Chem 68:1465–1473.
Harvey DJ. 1999. Matrix-assisted laser desorption/ionization mass spectrometry of carbohydrates. Mass Spectrom Rev 18:349–451.
Hassel T, Gleave S, Butler M. 1991. Growth inhibition in animal cell culture: the effect of lactate and ammonia. Appl Biochem Biotechnol 30:29–41.
Hayter PM, Curling EMA, Gould ML, Bains AJ, Jenkins N, Salmon I, Strange PG, Tong JM, Bull AT. 1992. Glucose-limited chemostat culture of Chinese hamster ovary cells producing recombinant human interferon-γ. Biotechnol Bioeng 39:327–335.
Hooker AD, James DC. 1998. The glycosylation heterogeneity of recombinant human IFN-gamma. J Interferon Cytokine Res 18:287–295.
Hooker AD, James DC. 2000. Analysis of glycoprotein heterogeneity by capillary electrophoresis and mass spectrometry. Mol Biotechnol 14:241–249.
Hooker AD, Goldman MH, Markham NH, James DC, Ison AP, Bull AT, Jenkins N. 1995. N-glycans of recombinant human interferon-gamma change during batch culture of Chinese hamster ovary cells. Biotechnol Bioeng 48:639–648.
Hooker AD, Green NH, Baines AJ, Bull AT, Jenkins N, Strange PG, James DC. 1999. Constraints on the transport and glycosylation of recombinant IFN-gamma in Chinese hamster ovary and insect cells. Biotechnol Bioeng 63:559–572.
James DC, Freedman RB, Hoare M, Jenkins N. 1994. High-resolution separation of recombinant human interferon-gamma glycoforms by micellar electrokinetic capillary chromatography. Anal Biochem 222: 315–322.
James DC, Freedman RB, Hoare M, Ogonah OW, Rooney BC, Larionov OA. 1995. N-glycosylation of recombinant human interferon-gamma produced in different animal expression systems. Biotechnology 13: 592–596.
Jenkins N, Parekh RB, James DC. 1996. Getting the glycosylation right-implications for the biotechnology industry. Nat Biotechnol 14: 975–981.
Kelker HC, Yip YK, Anderson P, Vilcek J. 1983. Effects of glycosidase treatment on the physicochemical properties and biological activity of human interferon gamma. J Biol Chem 258:8010–8013.
Kornfeld R, Kornfeld S. 1985. Assembly of asparagines-linked oligosaccharides. Annu Rev Biochem 54:631–664.
Lao MS, Toth D. 1997. Effects of ammonium and lactate on growth and metabolism of CHO cell culture. Biotechnol Prog 13:688–691.
Lee YY, Yap MGS, Hu WS, Wong KTY. 2003. Low-glutamine fed-batch cultures of 293-HEK serum-free suspension cells for adenovirus production. Biotechnol Prog 19:501–509.
Ljunggren J, Haggstrom L. 1994. Catabolic control of hybridoma cells by glucose and glutamine limited fed batch cultures. Biotechnol Bioeng 44:808–818.
McKeehan WL. 1982. Gycolysis, glutaminolysis and cell proliferation. Cell Biol Int Rep 6:635–649.
Nyberg GB, Balcarcel RR, Follstad BD, Stephanapoulous G, Wang DIC. 1999. Metabolic effects on recombinant interferon-γ glycosylation in continuous culture of Chinese hamster ovary cells. Biotechnol Bioeng 62:336–347.
Parekh RB. 1991. Mammalian cell gene expression: protein glycosylation. Curr Opin Biotechnol 2:730–734.
Pels Rijcken WRP, Overdijk B, Vandeneijnden DH, Ferwerda W. 1995. The effect of increasing nucleotide sugar concentrations on the incorporation of sugars into glycoconjugates in rat hepatocytes. Biochem J 305:865–870.
Samuel CE. 1991. Antiviral actions of interferon. Interferon-regulated cellular proteins and their surprisingly selective antiviral activities. Virology 183:1–11.
Sareneva T, Pirhonen J, Cantell K, Kalkkinen N, Julkunen I. 1994. Role of N-glycosylation in the synthesis, dimerization and secretion of human interferon-gamma. Biochem J 303:831–840.
Sareneva T, Pirhonen J, Cantell K, Julkunen I. 1995. N-glycosylation of human interferon-gamma: glycans at Asn-25 are critical for protease resistance. Biochem J 308:9–14.
Sareneva T, Mortz E, Tolo H, Roepstorff P, Julkunen I. 1996. Biosynthesis and N-glycosylation of human interferon-gamma. Asn25 and Asn97 differ markedly in how efficiently they are glycosylated and in their oligosaccharide composition. Eur J Biochem 242:191–200.
Scahill SJ, Devos R, Der Heyden VJ, Fiers W. 1983. Expression and characterization of the product of a human immune interferon cDNA gene in Chinese hamster ovary cells. Proc Natl Acad Sci U S A 80: 4654–4658.
Strichman R, Samuel CE. 2001. The role of gamma interferon in antimicrobial immunity. Curr Opin Microbiol 4:251–259.
Urlaub G, Chasin LA. 1980. Isolation of Chinese hamster cell mutants deficient in dihydrofolate reductase activity. Proc Natl Acad Sci U S A 77:4216–4220.
Varki A. 1993. Biological roles of oligosaccharides: all of the theories are correct. Glycobiology 3:97–130.
Xie L, Nyberg G, Gu X, Li H, Mollborn F, Wang DIC. 1997. Gamma-interferon production and quality in stoichiometric fed-batch cultures of chinese hamster ovary cells under serum-free conditions. Biotechnol Bioeng 56:577–582.
Yang M, Butler M. 2000. Effects of ammonia on CHO cell growth, erythropoietin production and glycosylation. Biotechnol Bioeng 68: 370–380.
Yuk IH, Wang DI. 2002. Changes in overall extent of protein glycosylation by Chinese hamster ovary cells over the course of batch culture. Biotechnol Appl Biochem 36:133–140.
Zhou W, Rehm J, Hu WS. 1995. High viable cell concentration fed-batch cultures of hybridoma cells through on-line nutrient feeding. Biotechnol Bioeng 46:579–587.